# HOKKAIDO UNIVERSITY

Instructions for use

# Magnetic field induced insulator-to-metal Mott transition in λ-type organic conductors

S. Fukuoka⬤, T. Oka, Y. Ihara⬤, and A. Kawamoto⬤

*Department of Condensed Matter Physics, Graduate School of Science, Hokkaido University, Sapporo 060-0810, Japan*

S. Imajo⬤ and K. Kindo

*Institute for Solid State Physics, The University of Tokyo, Kashiwa, Chiba 277-8581, Japan*

The effects of a magnetic field on the Mott transition, a longstanding issue in condensed matter physics, are studied using magnetoresistance measurements for organic Mott insulators, λ-(BETS)$_2$GaBr$_x$Cl$_{4-x}$, up to 55 T. We demonstrate that an insulator-to-metal transition with a first-order nature and a successive superconductor-to-insulator-to-metal transition are induced by magnetic fields. We discuss the difference in magnetic susceptibility between the insulating and metallic phases, which is a key factor in inducing these transitions. Field induced transitions in experimentally feasible fields under ambient pressure conditions lead to further experimental verification of Mott transitions.

## I. INTRODUCTION

The Mott transition, which is a drastic change between electronic localization and delocalization, has been a central subject of research in condensed matter physics [1]. A wide variety of phenomena, including unconventional superconductivity and novel magnetic states, such as quantum spin liquid states, emerge in the vicinity of the Mott boundary [2–4]. In the Mott-insulating state, the charge degrees of freedom are frozen by Coulomb repulsion. A Mott transition can be induced by carrier doping or by applying pressure [5–7]. Because the Mott transition is caused by the competition between Coulomb energy and electronic kinetic energy, it is, in principle, insensitive to magnetic fields. However, enhanced magnetism in a strongly correlated electron system leads to the Zeeman effect competing with the relevant energy scale, resulting in a magnetic field induced Mott transition [3,8–11]. Theoretical studies have predicted that the magnetic susceptibility of a strongly correlated metal is enhanced by a magnetic field, and a further metamagnetic localization transition is induced [8,9]. Such magnetic field induced localization has been experimentally confirmed in the quasi-two-dimensional organic conductor, $\kappa$-(BEDT-TTF)$_2$Cu[N(CN)$_2$]Cl, where BEDT-TTF is bis(ethylenedithio)tetrathiafulvalene [11]. The molecular structure of BEDT-TTF is shown in Fig. 1(a). However, the opposite magnetic field induced delocalization transition has been reported in some materials, which is caused by the energy gain from the Zeeman energy or associated structural instability [3,12]. These suggest that the magnetic nature adjacent to the Mott boundary is an important factor for the effect of the magnetic field on the Mott transition and further comprehensive studies are required.

To thoroughly investigate the effects of the magnetic field on the Mott transition, it is necessary to apply a magnetic field comparable to the energy scale of the Mott gap. However, the energy scale of the Mott gap is typically much larger than that of experimentally available magnetic fields, which

has prevented a comprehensive discussion of magnetic field effects on the Mott transition. To overcome this problem, it is necessary to realize an electronic state near the Mott boundary where the Coulomb repulsion and electronic kinetic energy are comparable. Organic conductors are suitable targets for studying the effects of magnetic fields on the Mott transition. Because organic conductors form a crystal structure through weak van der Waals forces, the electronic state is sensitively affected by relatively moderate pressures, which allows us to tune the electronic state close to the Mott boundary. For example, a Mott transition is induced by applying a pressure of approximately 30 MPa to $\kappa$-(BEDT-TTF)$_2$Cu[N(CN)$_2$]Cl [13–15]. By precisely tuning the system to the Mott boundary using moderate pressure, a magnetic field induced metal-to-insulator (M-I) Mott transition was observed at approximately 10 T [11]. Furthermore, the chemical pressure effect caused by molecule or atom substitution allows the tuning of the electronic state. In $\kappa$-(BEDT-TTF)$_2$Cu[N(CN)$_2$]Br, in which the ground state is a superconducting state, the negative pressure effect is obtained by deuterating the ethylene groups at the edges of BEDT-TTF molecules, and the ground state can be changed to a Mott insulating state [16–18].

In this paper, we focused on the quasi-two-dimensional organic superconductor λ-(BETS)$_2$GaCl$_4$, which consists of organic donor molecules of BETS$^{0.5+}$, where BETS is bis(ethylenedithio)tetraselenafulvalene, and counteranions of GaCl$_4^-$ [19]. The molecular structure of BETS and the crystal structure of λ-(BETS)$_2$GaCl$_4$ are shown in Fig. 1. BETS has a molecular structure in which the four sulfur atoms in the TTF skeleton of BEDT-TTF are replaced by selenium atoms. Since the atomic radius of selenium atoms is larger than that of sulfur atoms, the overlap integral between BETS molecules is larger than that in BEDT-TTF molecules. This substitution works to stabilize the metallic state. The BETS molecules and GaCl$_4^-$ counteranions form two-dimensional layered structures that are stacked alternately. There are two crystallographically nonequivalent BETS molecules, which
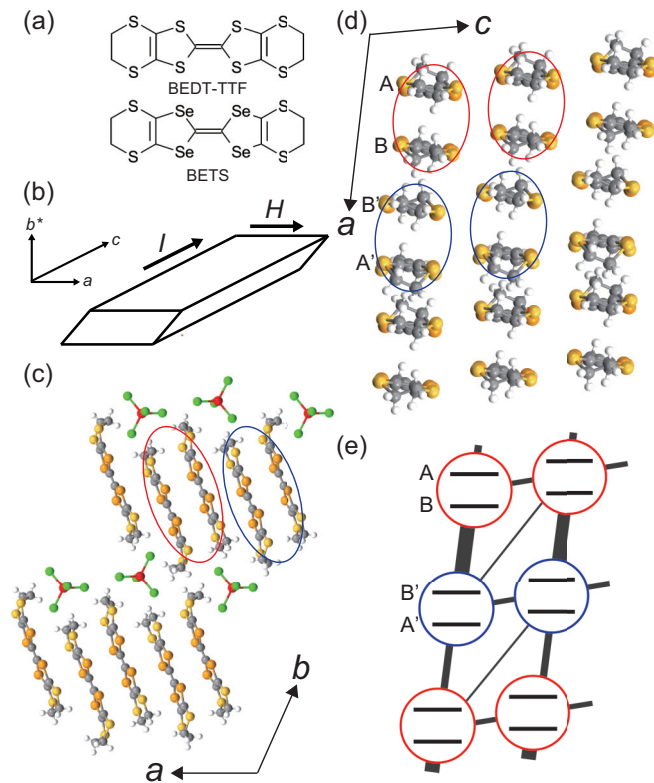
FIG. 1. (a) Molecular structures of BEDT-TTF and BETS. (b) A schematic drawing of the crystal shape of λ-type BETS salts. The direction of the applied current (*I*) and that of the applied magnetic field (*H*) are indicated by arrows. (c) The crystal structure of λ-(BETS)$_2$GaCl$_4$ viewed along the *c* axis. BETS molecules and GaCl$_4^-$ anions form layered structures separately and they stack along the *b* axis. The ellipsoids represent BETS dimers. (d) Molecular arrangement of the BETS molecules in the conduction layers. The blue and red ellipsoids represent the independent BETS dimers, which are related by inversion symmetry. (e) A schematic drawing of the conduction layers. The lines represent the interaction paths between the dimers, and the thickness of the lines represents schematically the strength of the interactions [20–22].



FIG. 2. *p*-*T* phase diagram of λ-(BETS)$_2$GaBr$_x$Cl$_{4-x}$. The red horizontal axis indicates the unit cell volume at room temperature [23]. The points marked with blue diamonds, green triangles, and red circles were determined in this study. The points marked with white diamonds, circles, triangles, and inverted triangles were determined by electrical resistivity and magnetic susceptibility measurements in previous studies [23].

are indicated as *A* and *B* in Fig. 1(d), and they form a dimer structure. *A'* and *B'* are crystallographically equivalent with *A* and *B*, respectively related by inversion symmetry. Figure 1(e) shows a schematic drawing of the molecular arrangement in the conduction layers. As GaCl$_4^-$ is a monovalent anion, a donor dimer has one hole, and the donor layers form an effective half-filled electronic state [20–22]. λ-(BETS)$_2$GaCl$_4$ shows a superconducting transition at 5.5 K. Unlike κ-type salts, in which the insulating phase adjacent to the Mott boundary is an antiferromagnetic insulating phase, the insulating phase adjacent to the Mott boundary in λ-type salts is suggested to be a nonmagnetic insulating or spin-density-wave (SDW) phase [23,24]. λ-type salts are important model materials for discussing the magnetic field effects on the Mott transition and its relationship with the magnetic state adjacent to the Mott boundary.

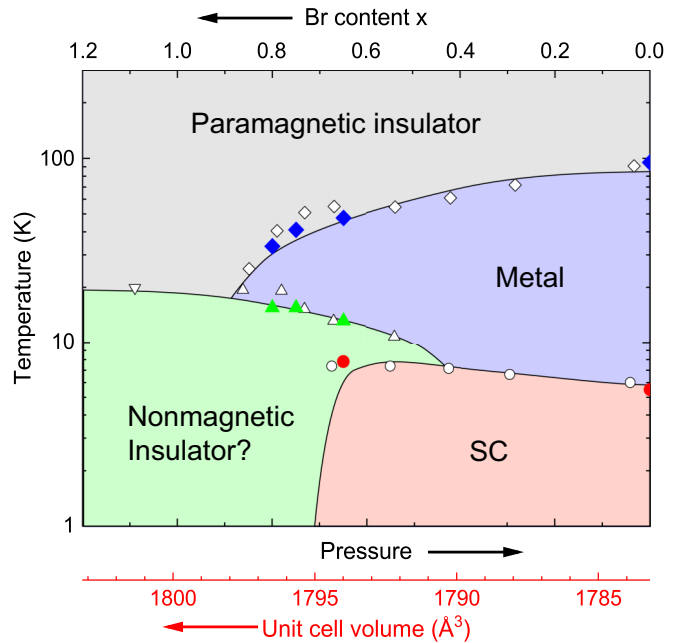For studying the magnetic field effects on the Mott transition, we focus on the anion substitution effect. Figure 2 shows the pressure-temperature (*p*-*T*) phase diagram of λ-type BETS salts [23]. The x-ray diffraction analysis for a series of λ-(BETS)$_2$GaBr$_x$Cl$_{4-x}$ confirmed that the unit cell volume increases linearly with increasing Br content following the formula $V = 1783.2 + 16.652x$, indicating that Br substitution gives rise to a negative chemical pressure effect [23]. Previous transport studies have revealed that the ground state changes from a superconducting state to an insulating state around $x = 0.75$ [23]. This suggests that the precise control of the Br content allows us to access the Mott boundary located around $x = 0.75$ under ambient conditions. This is advantageous for studying the magnetic field effects on the Mott transition because the field-temperature (*H*-*T*) phase diagram over wide temperature and magnetic field ranges can be investigated using pulsed high magnetic fields.

## II. EXPERIMENTAL

Single crystals of λ-(BETS)$_2$GaBr$_x$Cl$_{4-x}$ were grown by electrochemical oxidation of BETS in the presence of TBAGaCl$_4$ and TBAGaBrCl$_3$, where TBA is tetrabutylammonium, in an appropriate ratio in chlorobenzene. Compounds with $x = 0.65, 0.75$, and $0.8$ were prepared. λ-type BETS salts crystallize in the triclinic lattice and the long axis is parallel to the *c* axis. The crystal shape and crystal axis are shown in Fig. 1(b). The temperature dependence of the resistivity was measured using the four-terminal method with an ac current applied along the *c* axis. The magnetic field was set parallel to the conduction plane and perpendicular to the direction of the current as shown in Fig. 1(b) using a rotating sample holder. Magnetoresistance measurements were performed
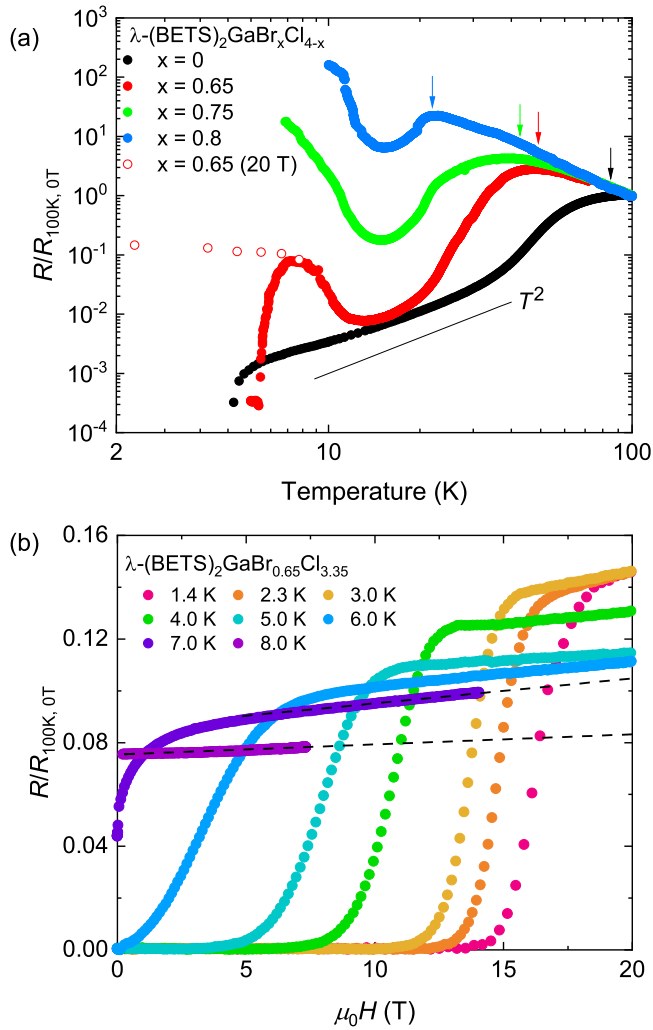
FIG. 3. (a) Temperature dependence of the scaled resistance $R/R_{100\,K,0\,T}$ of $\lambda$-(BETS)$_2$GaBr$_x$Cl$_{4-x}$. The open red symbols are the resistivity of the compound with $x = 0.65$ in the normal state at 20 T. (b) Magnetic field dependence of the resistivity of the compound with $x = 0.65$ measured up to 20 T at each temperature.

using a 60-T pulse magnet at the International MegaGauss Science Laboratory of the ISSP.

## III. RESULTS AND DISCUSSION

Figure 3(a) shows the temperature dependence of the resistivity scaled by the resistivity at 100 K. For comparison, the resistivity of $\lambda$-(BETS)$_2$GaCl$_4$ ($x = 0$) is also shown in the same figure [25]. In all the compounds, the resistivity exhibited an inflection point, and an insulator-to-metal crossover was observed at $T^*$, as indicated by the arrows in Fig. 3(a). In the case of $\lambda$-(BETS)$_2$GaCl$_4$, the temperature dependence of the resistivity is proportional to $T^2$, and $1/T_1T$ estimated by the $^{13}$C NMR measurements is constant below $T^*$, suggesting a Fermi-liquid state [26,27]. $T^*$ shifted to lower temperatures with increasing Br content. The resistivity decreased below $T^*$ for all the compounds and reached a minimum at approximately 15 K, which is defined as $T_{min}$. The $T^*$ and $T_{min}$ values for each compound determined in this study are plotted in
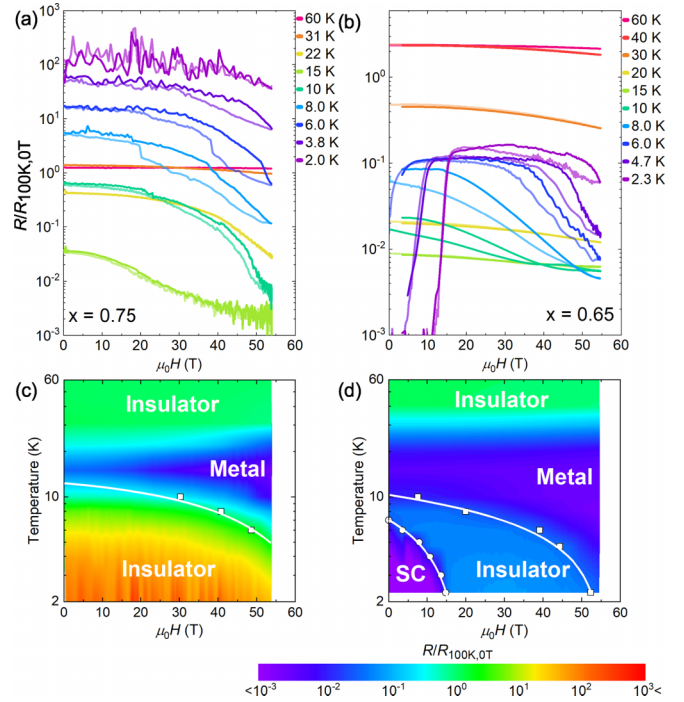


FIG. 4. (a), (b) Magnetic field dependence of the resistivity of the compound with $x = 0.75$ and 0.65 up to about 55 T. (c), (d) $H$-$T$ phase diagram of the compound with $x = 0.75$ and 0.65. The colors correspond to the value of the resistivity.

Fig. 2 by blue diamonds and green triangles, respectively. Our results are in good agreement with those of previous studies [23].

For the compound with $x = 0.65$, a sharp resistivity drop was observed at 7.6 K. Figure 3(b) shows the magnetoresistance of the compound with $x = 0.65$ measured up to 20 T at several temperatures below 8 K. A sharp increase in resistivity was observed with the application of a magnetic field, suggesting that the resistivity drop at zero field can be attributed to a superconducting transition. We evaluated the resistivity in the normal state without superconductivity using the resistivity at 20 T above the critical magnetic field ($H_{c2}$). The resistivities at 7 and 8 K at 20 T were estimated by extrapolating the resistivity in the normal state. The dashed lines in Fig. 3(b) indicate the extrapolation of the resistivity in the normal state. The red open circles in Fig. 3(a) indicate the temperature dependence of the resistivity at 20 T. The resistivity at 20 T increases toward lower temperatures, as in other compounds, indicating that the compound with $x = 0.65$ is also insulating when the superconductivity is suppressed. The decrease in resistivity originated from the growth of percolated superconducting domains in the dominant insulating phase, and the insulating behavior was restored by the breakdown of the superconducting state by a magnetic field. These results suggest that the compound with $x = 0.65$ is located on the insulator side, close to the Mott boundary.

To investigate the effects of the magnetic field on the Mott transition, magnetoresistance measurements were performed up to 55 T. Figures 4(a) and 4(b) show the temperature dependence of the magnetoresistance for compounds with $x = 0.75$ and 0.65. The magnetoresistance in the upward and downward

magnetic field sweeps is indicated by the dark and light lines, respectively. Negative magnetoresistance was observed at all temperatures. Above $T_{min}$, a small magnetoresistance without hysteresis was observed. In contrast, the magnitude of the negative magnetoresistance increased significantly near $T_{min}$. In the insulating phase below $T_{min}$, a sharp drop in resistivity was observed above a certain magnetic field, which is defined as $H_{IM}$, and hysteresis was clearly observed. The sharp resistivity drop with hysteresis can be interpreted as a first-order magnetic field induced insulator-to-metal (I-M) transition. In the compound with $x = 0.65$, a suppression of the superconducting state was observed at low fields below 8 K, and a sharp resistance drop with a first-order nature occurred at high fields, indicating a successive superconductor-to-insulator-to-metal (SC-I-M) transition.

The results of the magnetoresistance measurements are summarized as color plots of the $H$-$T$ phase diagram in Figs. 4(c) and 4(d). The observation of the magnetic field induced I-M transition suggests that the first-order Mott boundary in the $p$-$T$ phase diagram shifts to the lower-pressure side by the magnetic field, and the difference in $H_{IM}$ depending on the Br content is attributed to the fact that the compound with a higher Br content is farther from the boundary.

Near the Mott boundary, the Coulomb and kinetic energies are comparable, resulting in a small Mott gap. Therefore, the electronic state can be changed with a relatively small energy gain, owing to the Zeeman effect. As the electronic state shifts away from the Mott boundary to the insulator side, namely, as the Br content increases, the effective Mott gap increases, requiring a larger magnetic field to induce the I-M Mott transition. The absence of a phase transition at temperatures above $T_{min}$ can be explained by the fact that both compounds are in the metal phase or crossover region above the critical endpoint. Similar behavior has also been observed for $\kappa$-type salts [11]. In this case, the metallic state can be stabilized, but the electronic system does not cross the first-order Mott boundary and instead undergoes a continuous crossover.

Our results reveal that magnetic fields stabilize the metallic ground state rather than the insulating state in $\lambda$-type salts. This result is in stark contrast to the field induced localization observed in $\kappa$-type salts [8,9]. As a possible scenario for the opposite magnetic field responses of $\lambda$- and $\kappa$-type salts, we propose a magnetic free energy gain originating from the difference in the magnetization of the metal and insulator phases ($\Delta M = M_{ins} - M_{metal}$). From a thermodynamic viewpoint, a spin system prefers a larger magnetization in a magnetic field. Previously, a similar magnetic field induced I-M Mott transition was observed in EtMe$_3$P[Pd(dmit)$_2$]$_2$, where Et and Me denote $C_2H_5$ and $CH_3$, respectively, and dmit is 1,3-dithiole-2-thione-4,5-dithiolate [3]. EtMe$_3$P[Pd(dmit)$_2$]$_2$ exhibits a valence-bond solid phase with a nonmagnetic nature adjacent to the Mott boundary, and a magnetic field induced I-M Mott transition with discontinuous jumps in resistance was observed in magnetoresistance measurements [3]. In the case of $\kappa$-type salts, the Fermi-liquid state (paramagnetic metal or superconductivity) is adjacent to the antiferromagnetic (weak ferromagnetic) Mott insulating phase at low temperatures, and the magnetization of the insulating phase is greater than that of the metal phase ($\Delta M > 0$), resulting in the stabilization of
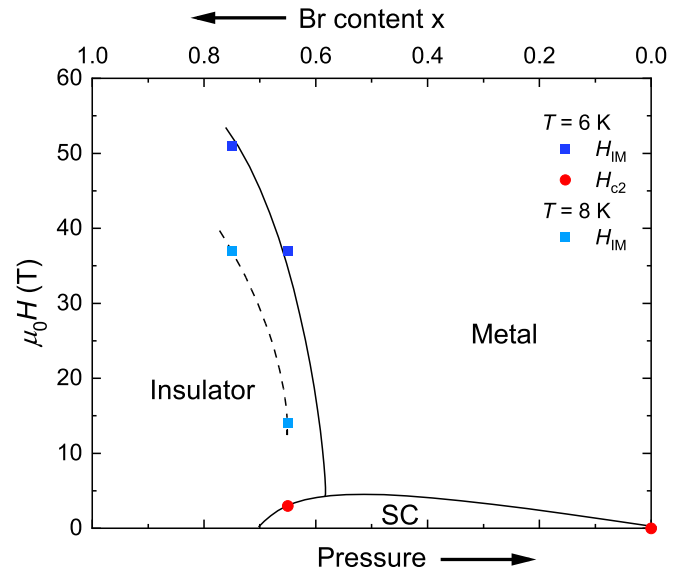


FIG. 5. *p-H* phase diagram at 6 K (solid line) and 8 K (dashed line).

the insulator phase in a magnetic field [28,29]. In contrast, the magnetic susceptibility of $\lambda$-(BETS)$_2$GaBr$_x$Cl$_{4-x}$ is found to decrease with increasing Br content at low temperatures; that is, $\Delta M < 0$ [23]. Thus, the metal phase can be stabilized in strong magnetic fields, leading to the magnetic field induced I-M Mott transition. The difference in magnetic susceptibility between compounds with different Br content becomes small with increasing temperatures. This can explain the small magnetoresistance at high temperatures because the energy gain from the Zeeman effect is small.

For $\kappa$-type salts, it is difficult to measure magnetic susceptibility under pressure, which prevents experimental investigations near the Mott boundary [3,11]. In $\lambda$-type salts, on the other hand, quantitative evaluation of the magnetic susceptibility very close to the Mott boundary is possible by using the chemical pressure effects. Figure 5 shows the pressure-magnetic field ($p$-$H$) phase diagrams of the $\lambda$-type salts at 6 and 8 K below $T_{min}$ determined from the results shown in Figs. 4(a) and 4(b). Since a linear relationship between Br content and unit cell volume has been confirmed, the horizontal axis can be regarded as effective pressure [23]. $H_{IM}$ was defined as the point at which a resistance drop was observed in the upward-field-sweep process. Our results confirm that the slope of the phase transition line between the insulator and metal phases in the $\lambda$-type salt is negative. This is in contrast to the case in $\kappa$-(BEDT-TTF)$_2$Cu[N(CN)$_2$]Cl that the slope of the phase transition line is positive [11]. From the Clausius-Clapeyron relation, the slope of the phase boundary can be written as

$$\frac{dH}{dp} = \frac{\Delta V}{\Delta M} = \frac{V_{ins} - V_{metal(SC)}}{M_{ins} - M_{metal(SC)}}, \quad (1)$$

where $\Delta V$ is the difference between the volumes in the insulating state ($V_{ins}$) and metal (SC) state ($V_{metal(SC)}$). Because the insulating phase is located on the negative-pressure side of the metal and superconductor phases, $\Delta V$ is positive, assuming that the cell volume is almost unchanged by

the magnetic field. The smaller magnetization in a larger Br content compound yields a negative $\Delta M$. Therefore, the Clausius-Clapeyron relation implies that the slope of the phase boundary is negative ($\Delta V / \Delta M < 0$), which is consistent with our experimental results [23].

Comparing the insulator and superconductor phases, the magnetic susceptibility in the superconductor phase is negative owing to the Meissner effect, suggesting that the slope of the phase transition line between the insulator and superconductor phases is positive ($\Delta V / \Delta M > 0$) and that an inflection point exists. The successive SC-I-M transitions can be induced by choosing the appropriate pressure or Br content, which corresponds to the result of the compound with $x = 0.65$ in this study.

Our results confirmed that $\lambda$-type salts exhibit magnetic field responses opposite to those of $\kappa$-type salts and imply that the smaller magnetic susceptibility in the insulator phase in $\lambda$-type salts may play a key role. As the cause of the reduction of the magnetization in the insulator phase, we point out that several magnetic phases compete near the Mott boundary in $\lambda$-type salts. While the insulator phase adjacent to the Mott boundary is antiferromagnetic phase for many Mott insulators including $\kappa$-type salts, that in $\lambda$-type salts is proposed to be a nonmagnetic phase, because the decrease in the magnetic susceptibility was observed in $\lambda$-(BETS)$_2$GaBr$_x$Cl$_{4-x}$ with a larger $x$ ($x \geqq 1.0$) [23,30,31]. As shown in Figs. 1(d) and 1(e), dimerized BETS molecules are stacked in the $a$-axis direction in the donor layers unlike $\kappa$-type salts, and a one-dimensional nature appears in the electronic structure. Theoretical studies considering the electronic structure of $\lambda$-type salts suggest that effective Heisenberg coupling alternates along the $a$ axis, and that the antiferromagnetic phase competes with the spin-gap phase [32,33]. On the other hand, the recent $^{13}$C NMR measurements for $\lambda$-(BETS)$_2$GaBr$_{0.75}$Cl$_{3.25}$ suggest the possible existence of an SDW phase in a very small area in the vicinity of the boundary. Since the band calculation confirmed that $\lambda$-type salts have multiband Fermi surfaces with quasi-one-dimensional and quasi-two-dimensional natures, the nesting instability in the quasi-one-dimensional Fermi surface can cause the SDW transition [20–22]. We speculate that such competition of the magnetic states could cause the reduction of the magnetization in the insulator phase and should be taken into account to explain the magnetic field effects on the Mott transition in $\lambda$-type salts. To achieve microscopic elucidation of the magnetic field effects on the Mott transition, we believe that further theoretical studies incorporating the effect of electron correlation in accordance with actual materials are needed.

## IV. CONCLUSION

In conclusion, we investigated the magnetic field effects on the Mott transition for $\lambda$-type salts using pulsed magnetic fields up to approximately 55 T and established the *p-H* and *H-T* phase diagrams over wide temperature and magnetic field ranges around the Mott boundary. The $\lambda$-type salts exhibited a magnetic field induced insulator-to-metal transition. We also detected a successive superconductor-to-insulator-to-metal transition for the compound with $x = 0.65$, which was located close to the Mott boundary. Such magnetic field dependence can be attributed to the unconventional insulator phase with a small magnetic susceptibility.

[1] N. F. Mott, *Metal-Insulator Transitions* (Taylor & Francis, London, 1990).

[2] K. Kanoda, Hyperfine Interact. **104**, 235 (1997).

[3] Y. Shimizu, H. Akimoto, H. Tsujii, A. Tajima, and R. Kato, Phys. Rev. Lett. **99**, 256403 (2007).

[4] T. Itou, A. Oyamada, S. Maegawa, M. Tamura, and R. Kato, Phys. Rev. B **77**, 104413 (2008).

[5] A. Jayaraman, D. B. McWhan, J. P. Remeika, and P. D. Dernier, Phys. Rev. B **2**, 3751 (1970).

[6] D. B. McWhan, T. M. Rice, and J. P. Remeika, Phys. Rev. Lett. **23**, 1384 (1969).

[7] D. B. McWhan and J. P. Remeika, Phys. Rev. B **2**, 3734 (1970).

[8] A. Georges, G. Kotliar, W. Krauth, and M. J. Rozenberg, Rev. Mod. Phys. **68**, 13 (1996).

[9] L. Laloux, A. Georges, and W. Krauth, Phys. Rev. B **50**, 3092 (1994).

[10] F. Kagawa, T. Itou, K. Miyagawa, and K. Kanoda, Phys. Rev. B **69**, 064511 (2004).

[11] F. Kagawa, T. Itou, K. Miyagawa, and K. Kanoda, Phys. Rev. Lett. **93**, 127001 (2004).

[12] Y. H. Matsuda, D. Nakamura, A. Ikeda, S. Takeyama, Y. Suga, H. Nakahara, and Y. Muraoka, Nat. Commun. **11**, 3591 (2020).

[13] S. Lefebvre, P. Wzietek, S. Brown, C. Bourbonnais, D. Jérome, C. Mézière, M. Fourmigué, and P. Batail, Phys. Rev. Lett. **85**, 5420 (2000).

[14] P. Limelette, P. Wzietek, S. Florens, A. Georges, T. A. Costi, C. Pasquier, D. Jérome, C. Mézière, and P. Batail, Phys. Rev. Lett. **91**, 016401 (2003).

[15] D. Fournier, M. Poirier, M. Castonguay, and K. D. Truong, Phys. Rev. Lett. **90**, 127002 (2003).

[16] A. Kawamoto, H. Taniguchi, and K. Kanoda, J. Am. Chem. Soc. **120**, 10984 (1998).

[17] H. Taniguchi, K. Kanoda, and A. Kawamoto, Phys. Rev. B **67**, 014510 (2003).

[18] Y. Matsumura, S. Imajo, S. Yamashita, H. Akutsu, and Y. Nakazawa, Crystals **12**, 2 (2022).

[19] A. Kobayashi, T. Udagawa, H. Tomita, T. Naito, and H. Kobayashi, Chem. Lett. **22**, 2179 (1993).

[20] L. Montgomery, T. Burgin, J. Huffman, J. Ren, and M.-H. Whangbo, Physica C: Supercond. **219**, 490 (1994).

[21] C. Mielke, J. Singleton, M.-S. Nam, N. Harrison, C. C. Agosta, B. Fravel, and L. K. Montgomery, J. Phys.: Condens. Matter **13**, 8325 (2001).

[22] H. Aizawa, T. Koretsune, K. Kuroki, and H. Seo, J. Phys. Soc. Jpn. **87**, 093701 (2018).

[23] H. Tanaka, A. Kobayashi, A. Sato, H. Akutsu, and H. Kobayashi, J. Am. Chem. Soc. **121**, 760 (1999).

[24] T. Kobayashi, T. Ishikawa, A. Ohnuma, M. Sawada, N. Matsunaga, H. Uehara, and A. Kawamoto, Phys. Rev. Res. **2**, 023075 (2020).

[25] S. Imajo, T. Kobayashi, A. Kawamoto, K. Kindo, and Y. Nakazawa, Phys. Rev. B **103**, L220501 (2021).

[26] T. Kobayashi and A. Kawamoto, Phys. Rev. B **96**, 125115 (2017).

[27] S. Uji, K. Kodama, K. Sugii, T. Terashima, T. Yamaguchi, N. Kurita, S. Tsuchiya, T. Konoike, M. Kimata, A. Kobayashi, B. Zhou, and H. Kobayashi, J. Phys. Soc. Jpn. **84**, 104709 (2015).

[28] K. Miyagawa, A. Kawamoto, Y. Nakazawa, and K. Kanoda, Phys. Rev. Lett. **75**, 1174 (1995).

[29] F. Kagawa, Y. Kurosaki, K. Miyagawa, and K. Kanoda, Phys. Rev. B **78**, 184402 (2008).

[30] H. Kobayashi, H. Akutsu, E. Arai, H. Tanaka, and A. Kobayashi, Phys. Rev. B **56**, R8526 (1997).

[31] H. Kobayashi, E. Arai, T. Naito, H. Tanaka, A. Kobayashi, and T. Saito, Synth. Met. **85**, 1463 (1997).

[32] H. Seo and H. Fukuyama, J. Phys. Soc. Jpn. **66**, 3352 (1997).

[33] H. Seo and H. Fukuyama, Synth. Met. **103**, 1951 (1999).